# Computational design support for double-skin facades with concomitant acoustical protection and natural ventilation capability

Ardeshir Mahdavi, Josef Lechleitner, Egzon Bajraktari
TU Wien, Vienna, Austria

## Abstract

This paper presents an empirically-based grey-box approach toward estimating the sound insulation of a double-skin façade (DSF) with openings for natural ventilation. A manageable number of input variables pertaining to DSF's geometric and material attributes facilitate the computation of frequency-dependent and weighted sound reduction index values of the DSF. The resulting functionality can aid designers and engineers toward developing and accessing various configurational options regarding DSFs with combined ventilation effectiveness and acoustical protection.

## Introduction and background

Natural ventilation in buildings is typically realized via openings in the building enclosure. As a matter of course, the maximum sound insulation level of the building envelope is achieved when all openings are closed. This implies that

*i)* natural ventilation via envelope openings and

*ii)* envelope's sound insulation capacity

can represent conflicting envelope design objectives. In fact, aside from location-dependent outdoor thermal and air quality constraints, noise exposure may be the main factor preventing the inhabitants from using windows as means of ventilation. Consequently, arguments pertaining to noise control have been frequently used to justify a sealed building enclosure and exclusive reliance on mechanical ventilation. This circumstance is, however, problematic, as natural ventilation via window operation can effectively support the provision of fresh air to the indoor environments.

The present contribution thus addresses computational design support for a double-skin façade (DSF) with concomitant acoustical protection and natural ventilation capability. However, note that the achieving a high sound insulation level of building facades is not meant here as a solution to undue environmental noise exposure (due, for example, to excessive traffic): From a human-ecological perspective, such exposure issues need to be treated at the source (e.g., via traffic quietening measures), not at the receiver (Mahdavi 1996, 1986). In other words, in case of traffic noise exposure, emission-oriented measures (i.e., traffic quietening) are decidedly superior to immission-oriented ones (i.e., inoperable sound-insulating windows).

Nonetheless, building enclosure elements arguably need to exhibit a reasonable level of sound insulation, even for buildings in acoustically relative benign contextual circumstances.

Various aspects of building enclosure acoustics and natural ventilation have been explored in the past (see, for example, Buratti 2002, De Salis et al. 2002, Field & Fricke 1995, Khalegi et al. 2007, Mahdavi 1993, Mingeron & Potvin 2012, Nunes et al. 2010, Oldham et al. 2004, Viveiros & Gibbs 1997). However, there is still a need for reliable methods and tools to support the design and configuration of building enclosure components and systems that could accommodate, among other things, natural ventilation and sound insulation requirements.

In this context, the present contribution reports on the concluding findings of our research efforts (Mahdavi et al. 2013, 2012, Bajraktari et al. 2015a) for the experimental exploration of the potential of DSFs to support natural ventilation while maintaining sufficient levels of acoustical insulation.

In the course of this research, we empirically examined the influence of a number of factors (such as the geometric layout of the openings in the DSF's two layers and the deployment of acoustical absorption in the DSF's cavity) on the resulting sound insulation level. Moreover, we explored and evaluated the potential of both simple (empirically-based) calculation methods and detailed simulation approaches (Bajraktari et al. 2015b).

Specifically, we compared simulations and laboratory measurements pertaining to the sound insulation of an experimental DSF for multiple opening configurations. The results illustrate the potential as well as the considerable limitations of the state-of-art acoustical performance simulation tools toward prediction of the sound insulation of DSFs.

To further advance the existing predictive capabilities with regard to sound insulation of DSFs, we focus in this paper on the performance of an empirically-based grey-box model. Given the current state of art, this approach appears to be reasonable, as it can *i)* provide simple-to-use engineering design aides and *ii)* provide an empirically-based corrective in the development of future simulation tools for façade acoustics.

## Approach

### The experimental setting

To examine the accuracy of predictive models of DSFs' sound insulation, we constructed an experimental modular DSF with multiple opening possibilities installed in our laboratory (see Figure 1) placed in the opening between two adjacent reverberant chambers. The wall segment (dimensions 3.1 × 3.1 m) consists of two layers of chip-board panels mounted on aluminium bars. The distance (D) between the two layers amounts to 43 cm. In a 5 by 5 grid structure, each layer has 25 dismountable chip-board (0.5 by 0.5 m) square panels. Different numbers of elements can be opened in each layer, leading to different effective opening areas. Moreover, a number of elements embody smaller openings (50% and 25% of an element area, i.e., 0.125 and 0.0625 m²). Given the flexibility of the grid structure, the distance (d) between openings (see Figure 2) and thus the respective view factor and angle of sound diffraction can be varied. Likewise, the amount and location of cavity absorption can be changed via installation of modular sound absorption elements.

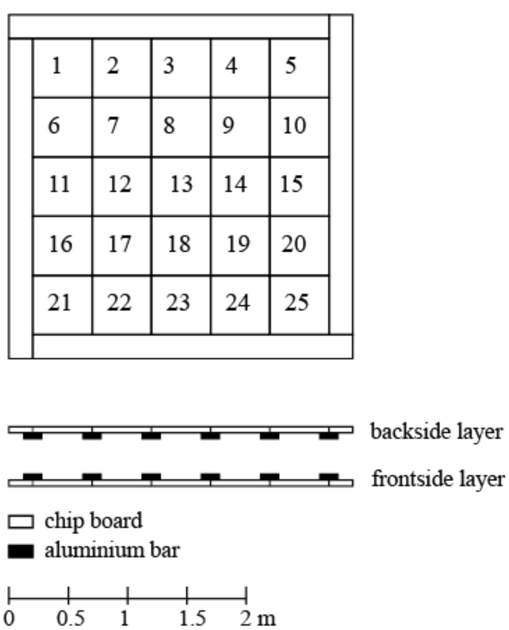


*Figure 1: Schematic illustration of the frontal view and plan of the experimental DSF.*

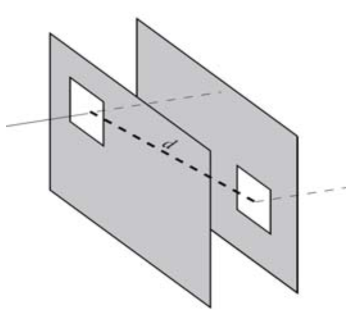


*Figure 2: Illustration of distance (d) between openings.*

Upon initial installation, the sound insulation of the construction was measured with first with one, and then with two layers fully closed. Subsequently, parametric laboratory measurements were conducted involving variations in opening size, displacement, and cavity absorption, resulting in frequency-dependent and weighted sound reduction index values. To process the results, we first considered a preliminary analytical models.

This model embodies a number of variables that are hypothesised to correlate with the resulting sound insulation level of DSFs with openings for natural ventilation. In a second step, we deployed advanced data mining techniques to derive a finely tuned mathematical expression for the derivation of the façade's acoustical insulation from the aforementioned candidate independent variables.

### Parametric measurements

Altogether, 176 different configurations were empirically studied. Table 1 shows a sample of these configurations. Figure 3 shows the respective distribution of effective opening areas. The measurement results were expressed in terms of frequency-dependent $R_f$ and weighted $R_w$ sound reduction indices (see ISO 2011, 2010).

### A simple analytical description

To identify the relevant independent variables influencing the resulting acoustical behaviour of the experimental wall, a simple model was considered involving three fundamental sound transmission paths (see Figure 4).

The first path ($\tau_1$) pertains to direct sound transmission through both layers (see equation 1). Once elements are opened in the two layers, two further paths must be considered. Thereby, path 2 ($\tau_2$) refers to direct airborne sound transmission, whereas path 3 ($\tau_3$) involves multiple intermediate reflections within the cavity (see equations 2 and 3).

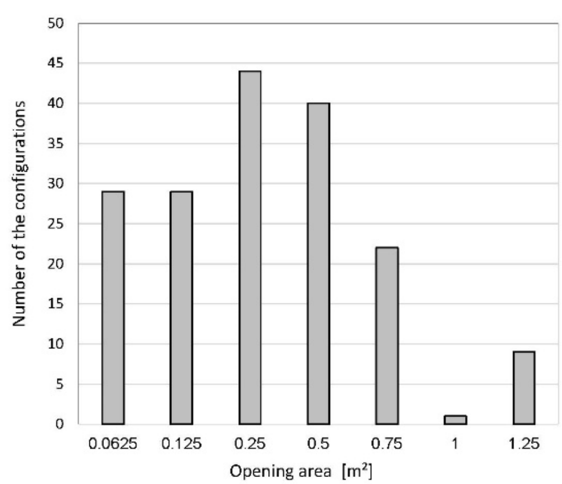


*Figure 3: Distribution of the effective opening areas considered in the course of parametric measurements.*

$$\tau_1 = \frac{W_{f,2}}{W_{f,1}} = 10^{-0.1 \cdot R_{f,\max}} \quad (1)$$

$$\tau_2 = \frac{W_{f,1} \cdot S_F \cdot VF}{W_{f,1}} \quad (2)$$

$$\tau_3 = \frac{W_{f,1} \cdot S_F \cdot (1-VF) \cdot (1-a_m)^n}{W_{f,1}} \quad (3)$$

In the above equations, $W_{f,1}$ and $W_{f,2}$ denote frequency-dependent sound energy density in source and receiver rooms respectively, $R_{f,\max}$ denotes, for a specific frequency $f$, the sound reduction index of the wall in fully closed state, $S_F$ denotes the area ratio of the opening area (toward the source room) and the wall's total area (i.e., $S_{open}/S_{ref}$), VF denotes the view factor (or shape factor) extended from the opening area in the source room to the opening area in the receiver room, $\alpha_m$ denotes the mean (area-weighted) cavity sound absorption, and n represents a factor corresponding to the number of reflections within the cavity.

Given this basic analytical description, the sound reduction index of a DSF with openings can be obtained from the source and receiver rooms' sound energy densities ($W_1$, $W_2$) as per equations 4 and 5:

$$R = -10 \cdot \log\left[\frac{W_2}{W_1}\right] \quad [\text{dB}] \quad (4)$$

$$R_f = -10 \cdot \log\left[10^{-0.1 \cdot R_{f,\max}} + S_F \cdot \left(VF + S_F \cdot (1-VF) \cdot (1-a_m)^n\right)\right] \quad [\text{dB}] \quad (5)$$

*Table 1: Selected instances from the list of configurations of the experimental DSF (the numeric code of the openable elements is shown in Figure 1). Distance d is shown in Figure 2. The minimum opening area in configurations 1 to 15 amounts to 0.25 m² (i.e., area of a modular openable element). Opening area in configuration 16 amounts to 0.0625 m² (i.e., 25% of the area of a modular 0.5 by 0.5 m element)*

| Config. number | Code of the open element in layer facing the source room | Element with added absorption in the cavity (on layer facing the source room) | Code of the open element in layer facing the receiver room | Element with added absorption in the cavity (on layer facing the receiver room) | Distance d (m) |
|---|---|---|---|---|---|
| 1 | - | - | - | - | |
| 2 | - | - | all | - | |
| 3 | 1 | - | 1 | - | 0.43 |
| 4 | 1 | - | 13 | - | 1.48 |
| 5 | 1 | - | 25 | - | 2.86 |
| 6 | 6, 16 | - | 6, 16 | - | 0.43 |
| 7 | 6, 16 | - | 8, 18 | - | 1.09 |
| 8 | 6, 16 | - | 10, 20 | - | 2.05 |
| 9 | 6, 16 | 2, 7, 12, 17, 22, 4, 9, 14, 19, 24 | 10, 20 | - | 2.05 |
| 10 | 6, 16 | 2, 7, 12, 17, 22, 4, 9, 14, 19, 24 | 10, 20 | 2, 7, 12, 17, 22, 4, 9, 14, 19, 24 | 2.05 |
| 11 | 1, 6, 11, 16, 21 | - | 1, 6, 11, 16, 21 | - | 0.43 |
| 12 | 1, 6, 11, 16, 21 | - | 3, 8, 13, 18, 23 | - | 1.09 |
| 13 | 1, 6, 11, 16, 21 | - | 5, 10, 15, 20, 25 | - | 2.05 |
| 14 | 1, 6, 11, 16, 21 | 2, 7, 12, 17, 22, 4, 9, 14, 19, 24 | 5, 10, 15, 20, 25 | - | 2.05 |
| 15 | 1, 6, 11, 16, 21 | 2, 7, 12, 17, 22, 4, 9, 14, 19, 24 | 5, 10, 15, 20, 25 | 2, 7, 12, 17, 22, 4, 9, 14, 19, 24 | 2.05 |
| 16 | 1 | 2, 7, 12, 17, 22, 4, 9, 14, 19, 24 | 25 | 2, 7, 12, 17, 22, 4, 9, 14, 19, 24 | 2.86 |

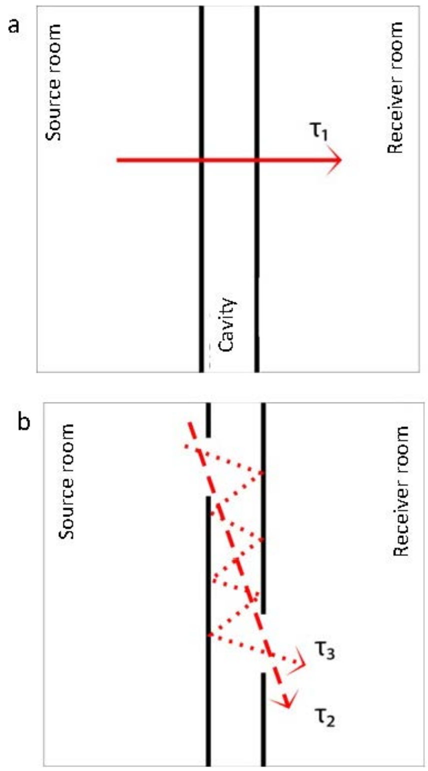


*Figure 4: Three basic sound transmission paths through a DSF with openings for natural ventilation: $\tau_1$ (a); $\tau_2$ and $\tau_3$ (b).*

Needless to say, the above formalism represents a stark simplification, as a number of salient factors (e.g., the stiffness of the individual layers or the frequency-dependent resonance phenomena) are not addressed. However, such factors play a lesser role in the resulting magnitude of sound insulation indicators, once elements are opened in the layers, leading to the dominance of paths 2 and 3 in the acoustical energy balance (see Figure 4). The above analytical formalism provides hence a convenient vehicle to identify hypothesised independent variables to be further scrutinised via empirical explorations.

## Results

### Basic sound insulation of the layers

To properly conduct and process parametric measurements, each of the two layers of the construction must display, in the fully closed state, a certain minimum level of sound insulation. As Figure 5 demonstrates, the measured sound reduction index of the experimental wall (with one and both layers fully closed) meet this requirement. The weighted sound reduction index ($R_w$) with only one fully closed layer amounts to 35 dB, whereas it amounts to 51 dB with both layers closed.

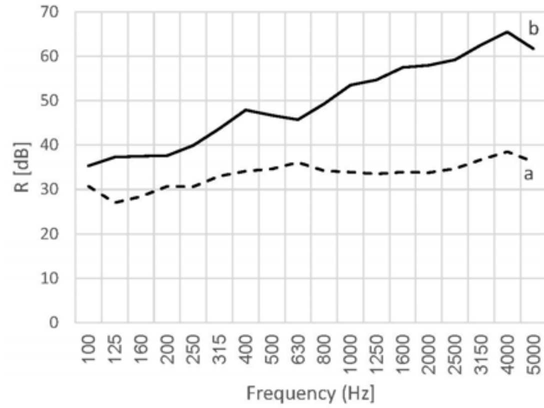


*Figure 5. Sound reduction index ($R_f$) of the experimental wall (a: one layer fully closed; b: both layers fully closed).*

### A grey-box model for the estimation of the frequency-dependent sound reduction index $R_f$

To process the parametric measurement results, we focused on the frequency-dependent reduction of the sound insulation index ($\Delta R_f$) of the fully closed construction as a consequence of opening various elements in the experimental wall. The advantage of this indicator lies in its relative nature and hence the potential for generalisation. In other words, other DSF constructions with known overall sound reduction index values can be analysed by applying reduction terms for different opening configurations. Specifically, the proposed reduction term denotes the difference between the frequency-dependent sound insulation index of the fully closed configuration ($R_{f,max}$) and that of a specific configuration ($R_f$):

$$\Delta R_f = R_{f,\max} - R_f \qquad \text{[dB]} \qquad (6)$$

The statistical analysis of the results led to the following simple formula for the computation of $\Delta R_f$:

$$\Delta R_f = 16.3 \cdot \log[f \cdot (1-\alpha_m) \cdot \cdot S_F \cdot \sqrt{\log(VF \cdot 10000)}] \qquad \text{[dB]} \qquad (7)$$

Figure 6 illustrates the level of agreement between measured $\Delta Rf$ values and those computed using equation 7.

Note that the computation of the variable VF in equation 7 can be rather cumbersome. We thus developed an alternative formulation as per equation 8.

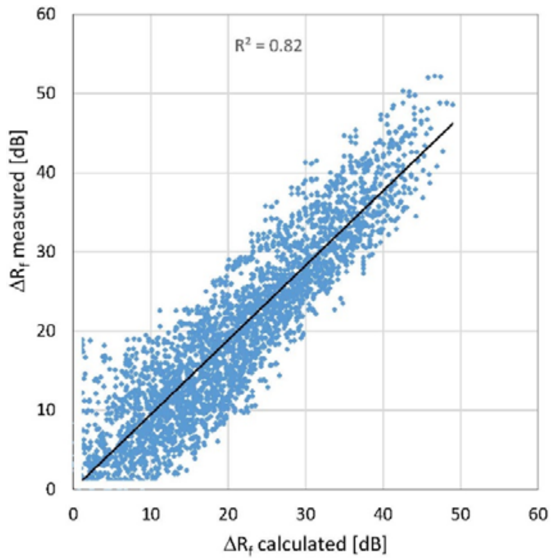


*Figure 6. Computed versus measured values of $\Delta R_f$.*

$$\Delta R_f = 16.3 \cdot \log\left[f \cdot G \cdot (1-\alpha_m)^3\right] + 9 \text{ [dB]} \quad (8)$$

Here, the variable G represents a kind of aggregate geometry factor as follows:

$$G = \frac{S_F \cdot D}{d} \quad (9)$$

Given an obtained value for $\Delta R_f$, $R_f$ can be simply calculated by rearranging Eq. 7:

$$R_f = R_{f,\max} - \Delta R_f \quad \text{[dB]} \quad (10)$$

**A grey-box model for the estimation of the weighted sound reduction index $R_w$**

A predictive model for the reduction of the weighted sound reduction index ($\Delta R_w$) of the fully closed DSF as a consequence of open elements can be established following a similar procedure (see the previous section). As such, this reduction term denotes the difference between the weighted insulation index of the fully closed configuration ($R_{w,max}$) and that of a specific configuration that includes openings ($R_w$):

$$\Delta R_w = R_{w,\max} - R_w \quad \text{[dB]} \quad (11)$$

In this case, the statistical analysis of the results yielded the relationship expressed in equation 12. Note that both calculated and measured values of $R_W$ were derived from the frequency-dependent values according to the procedure specified in the pertinent international standard (ISO 2011).

$$\Delta R_w = 10 \cdot \log[S_F \cdot \cdot \sqrt{VF} \cdot (1-\alpha_m)^3] + 50 \quad \text{[dB]} \quad (12)$$

Figure 7 illustrates the level of agreement between measured $\Delta R_w$ values and those computed using equation 12. Given a value for $\Delta R_w$, the respective value for $R_w$ can be obtained as follows:

$$R_w = R_{w,\max} - \Delta R_w \quad \text{[dB]} \quad (13)$$

Again, equation 12 requires the calculation of view factors. We thus derived also for this case an alternative formulation as follows:

$$\Delta R_w = 15.7 \cdot \log\left[G \cdot (1-\alpha_m)^3\right] + 56 \quad \text{[dB]} \quad (14)$$

Figure 8 graphically illustrates the relationships captured in equation 14.

**The reliability assessment of the computational results**

As mentioned before (see Figures 6 and 7), the computed results (R und $R_w$ values for configurations with openings) obtained from equations 10 and 13 were compared with laboratory measurements. Table 2 provides the results of the corresponding statistical assessment in terms of values for $R^2$ (coefficient of determination) und RMSE (root-mean-square error).

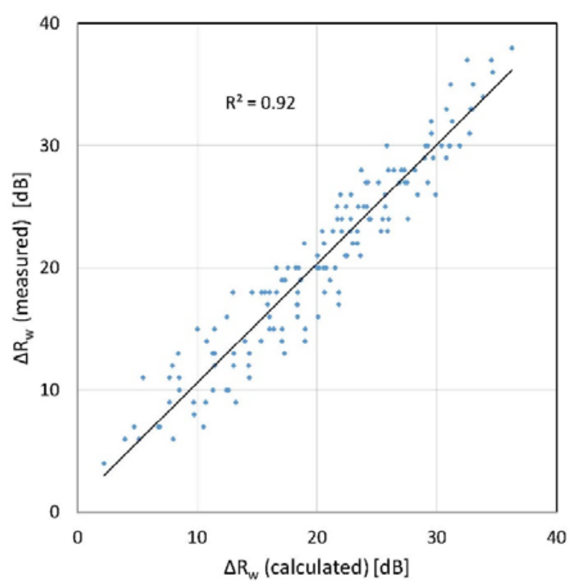


*Figure 7: Computed versus measured values of $\Delta R_w$*

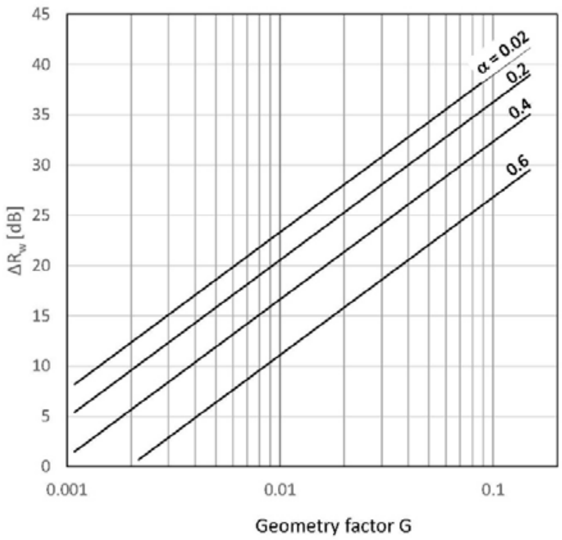


*Figure 8: Estimation of $\Delta R_w$ values as a function of the geometry factor G and mean cavity sound absorption coefficient $\alpha_m$.*

*Table 2: Statistical indicator values $R^2$ und RMSE pertaining to the comparison of computed and measured values of R and $R_W$*

| Computed parameter | Equation | $R^2$ | RMSE |
|---|---|---|---|
| $\Delta R_f$ | 7 | 0.82 | 4.9 |
| $R_f$ | 10 and 7 | 0.68 | 4.9 |
| $\Delta R_f$ | 8 | 0.86 | 4.1 |
| $R_f$ | 10 and 8 | 0.77 | 4.1 |
| $\Delta R_w$ | 12 | 0.92 | 2.2 |
| $R_w$ | 13 and 12 | 0.92 | 2.2 |
| $\Delta R_w$ | 14 | 0.92 | 2.3 |
| $R_w$ | 13 and 14 | 0.92 | 2.3 |

The relatively good performance of the proposed models is noteworthy, given the fact that they do not explicit include a number of potentially important influence factors such those pertaining to wave propagation phenomena and associated resonance behaviour. Specifically, computational estimations of the weighted sound reduction index $R_w$ were very close to the corresponding measured values. However, frequency-dependent sound insulation indices display larger errors, particularly in the lower frequency range. Be that as it may, the constraints involved in the experimental setup and the statistical treatment, the proposed empirically derived computational routines should be applied with care.

Specifically, the proposed formulas should be considered only if the weighted sound reduction index $R_w$ of the DSF under closed conditions displays a value of at least 40 dB. The ratio of the opening areas $S_F$ must be between 0.01 und 0.05. Likewise, the distance d between the opened elements should be at least 0.5 m and no larger than 3 m. Moreover, the distance D between the two layers should be between 0.3 and 1 m.

## Conclusion

We presented grey-box models for the estimation of the sound insulation of a DSF construction with openings for natural ventilation. Thereby, the objective was to support design methods that aim at facilitating natural ventilation while maintaining a sufficient level of acoustical insulation. Toward this end, we empirically studied a number of suspected influence factors pertaining to both geometry and material properties. As highly detailed first-principles based numeric methods are still not sufficiently mature and versatile enough to address practical queries, we focused our efforts on developing empirically-based grey-box models. Such models cannot only provide simple-to-use engineering design aides, but have also the potential to provide benchmarking data for supporting ongoing and future developments of numeric simulation tools for façade acoustics.

The supplied models facilitate the exploration of a number of relevant issues. For instance, the size of the openings and the positioning influence of the openings in the two layers relative to each other can be explored. Likewise, the effect of additional sound absorption in the cavity on the resulting sound insulation of the façade can be studied.

In future, we intend to address a number of limitations of the present study. A fundamental limitation pertains of course to the specific circumstances of our test DSF (e.g., overall size, distance between the two layers, specific construction of the constitutive elements). The current results thus cannot be unconditionally extrapolated to substantially different DSF constructions. A larger number of test specimens with differing dimensions and material properties would be needed to facilitate a more stringent verification and generalisation of the proposed models. A further interesting area of future inquiry would be the exploration of the dependency of air flow rates through the DSF on different opening configurations under standard boundary conditions.

## Acknowledgments

The research presented in this paper was supported in part by funds provided within the framework of the FFG ("die österreichische Forschungsförderungsgesellschaft") project "LEIse-Wand: Innovative Fassaden für natürliche Raumlüftung und optimierten Schallschutz" (project number 845179). The authors would also like to thankfully acknowledge the contributions by Ulrich Pont, Christian Steineder, and Nikolaus Maly toward data and text processing needed for this paper.

## References


Bajraktari, E., Lechleitner, J., and Mahdavi, A. (2015a). The Sound Insulation of Double Facades with Openings for Natural Ventilation. *Building Acoustics*, 22 (2015), 3+4; 163 - 176.

Bajraktari, E., Lechleitner, J., Mahdavi, A. (2015b). Estimating the sound insulation of double facades with openings for natural ventilation. *Energy Procedia* 78 (2015), pp. 140-145.

Buratti, C. (2002). Indoor noise reduction index with open window. *Applied Acoustics* 63 (63), pp. 431-451.

De Salis, M. H., Oldham, D. J., & Sharples, S. (2002). Noise control strategies for naturally ventilated buildings. *Building and Environment* 37. pp. 471-484.

Field, C. D., Fricke, F. R. (1995). The attenuation of road traffic noise entering buildings through ventilation openings using quarter wave resonators: mechanism of attenuation and model experiments. *Building Acous*tics 1995;2(4):625–35.

ISO (2010). EN ISO 10140-2: Acoustics – Laboratory measurement of sound insulation of building elements – Part 2: Measurement of airborne sound insulation.

ISO (2011). EN ISO 717-1: Acoustics – Rating of sound insulation in buildings and of building elements – Part 1: Airborne sound insulation (draft standard).

Khalegi, A., Bartlett, K., & Hodgson, M. (2007). Relationship between ventilation, air quality and acoustics in 'green' and 'brown' buildings. *19th International Congress of Acoustics*. Madrid.

Mahdavi, A. (1996). Approaches to Noise Control: A Human Ecological Perspective. Proceedings of the *NOISE-CON* 96. PP. 649-654.

Mahdavi, A. (1993). Thermal and Acoustical Performance of "Buffer Rooms". *ASHRAE Transactions*, Volume 99, Part 1. 1092 - 1105.

Mahdavi, A. (1986). Das Dilemma immissionsseitiger Lärmkontrolle. *Baumagazin*, 3/86 (1986), S. 134 - 138.

Mahdavi, A., Bajraktari, E., Hintermayer, M., and Lechleitner, J. (2013). Sound Insulation of Double Facades with Operable Windows: an Empirical Inquiry. *CLIMA 2013* World Congress. Society of Environmental Engineering, 1/1/1, Paper ID 275.

Mahdavi A., Çakir O., Pröglhöf C., & Lechleitner J. (2012). Sound insulation of a double-leaf wall system with openings for natural ventilation. Proceedings of the 5th International *Building Physics Conference* Kyoto, Japan (2012), pp. 1115 – 1118.

Migneron, J-P., Potvin, A. (2012). Noise reduction of a double-skin facade considering opening for natural ventilation. *Acoustics 2012* Hong Kong. J. Acoust. Soc. Am., Vol. 131, No. 4, Pt. 2, pp. 3320-3320.

Nunes, Z., Wilson, B., & Rickard, M. (2010). An assessment of the acoustic performance of open windows, in line with ventilation requirements for natural ventilation. *InterNoise* 2010.

Oldham, D. J., De Salis, M. H., & Sharples, S. (2004). Reducing the ingress of urban noise through natural ventilation openings. *Indoor Air* 14, pp. 118-126.

Viveiros, E.B., Gibbs, B.M. (1997). Sound insulation of ventilation louvres. Proceedings of *Internoise* '97. pp. 739–42.